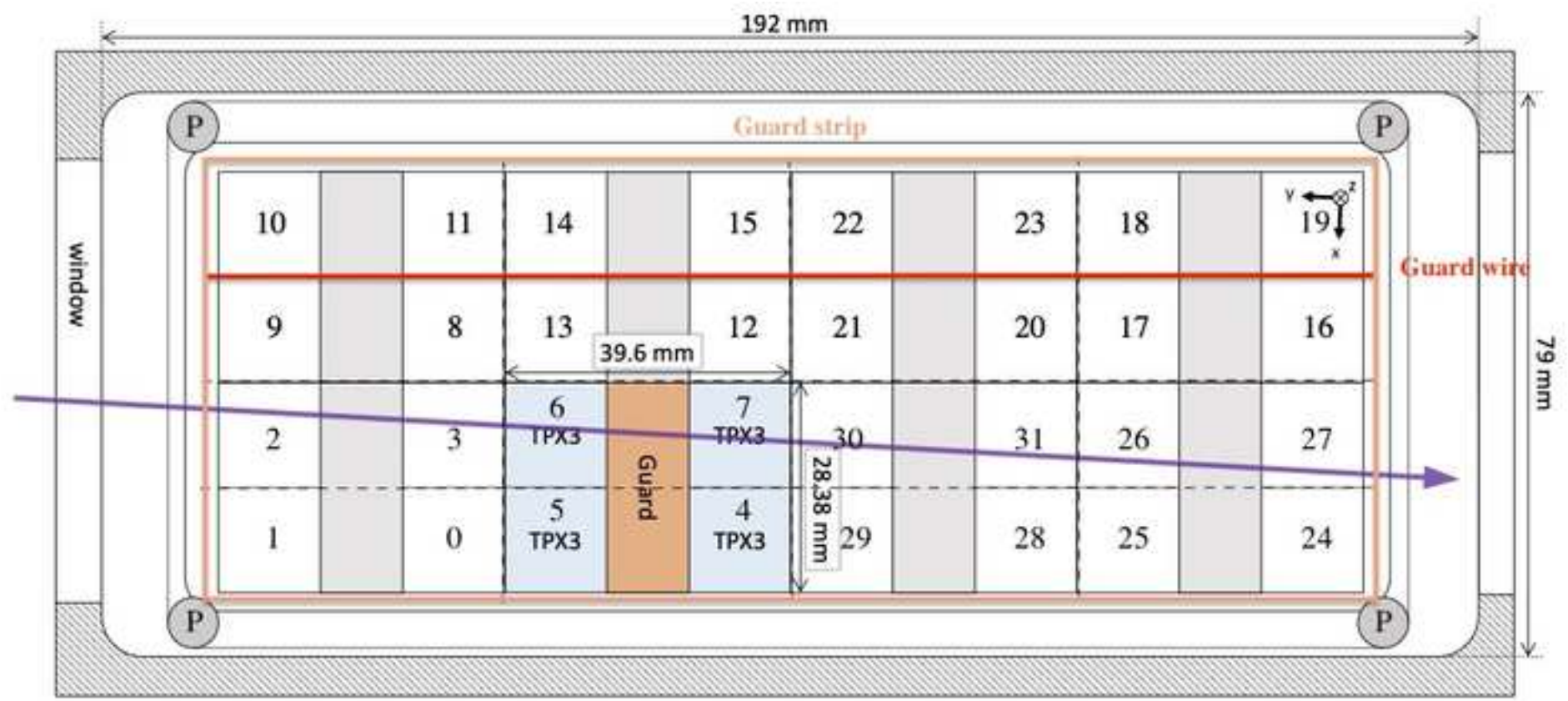


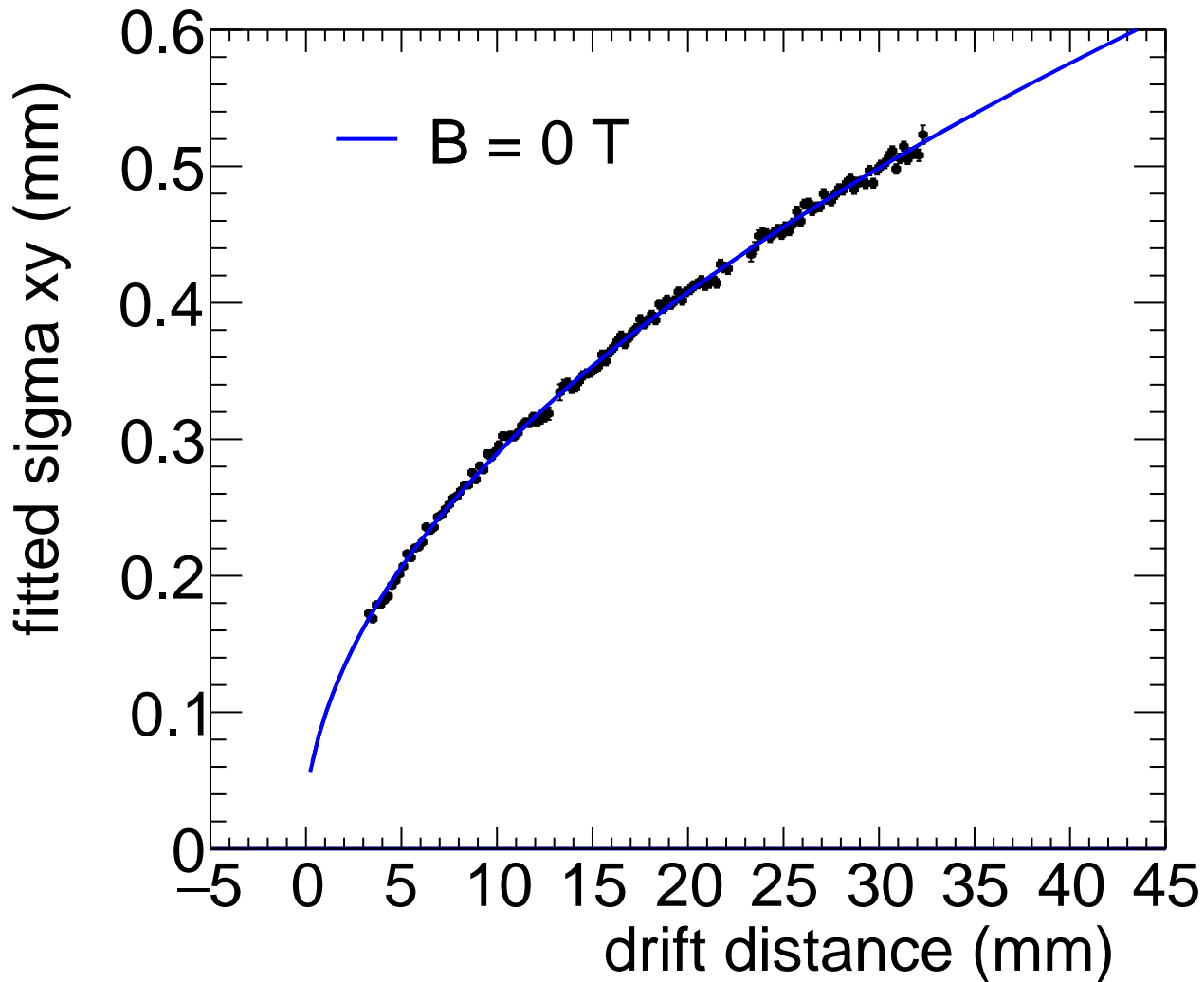
Nuclear Inst. and Methods in Physics Research, A

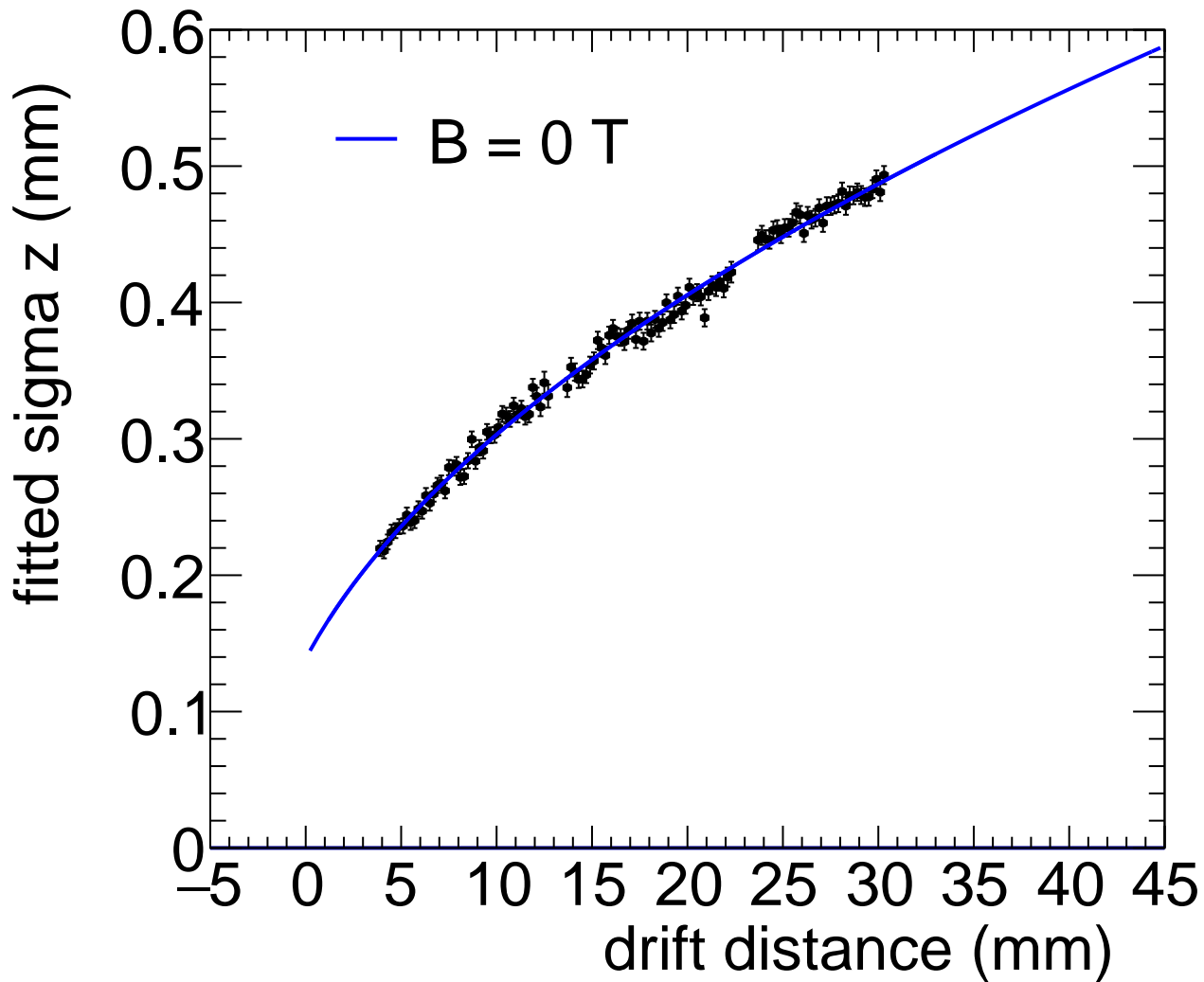
Towards a Pixel TPC part I: construction and test of a 32-chip GridPix detector

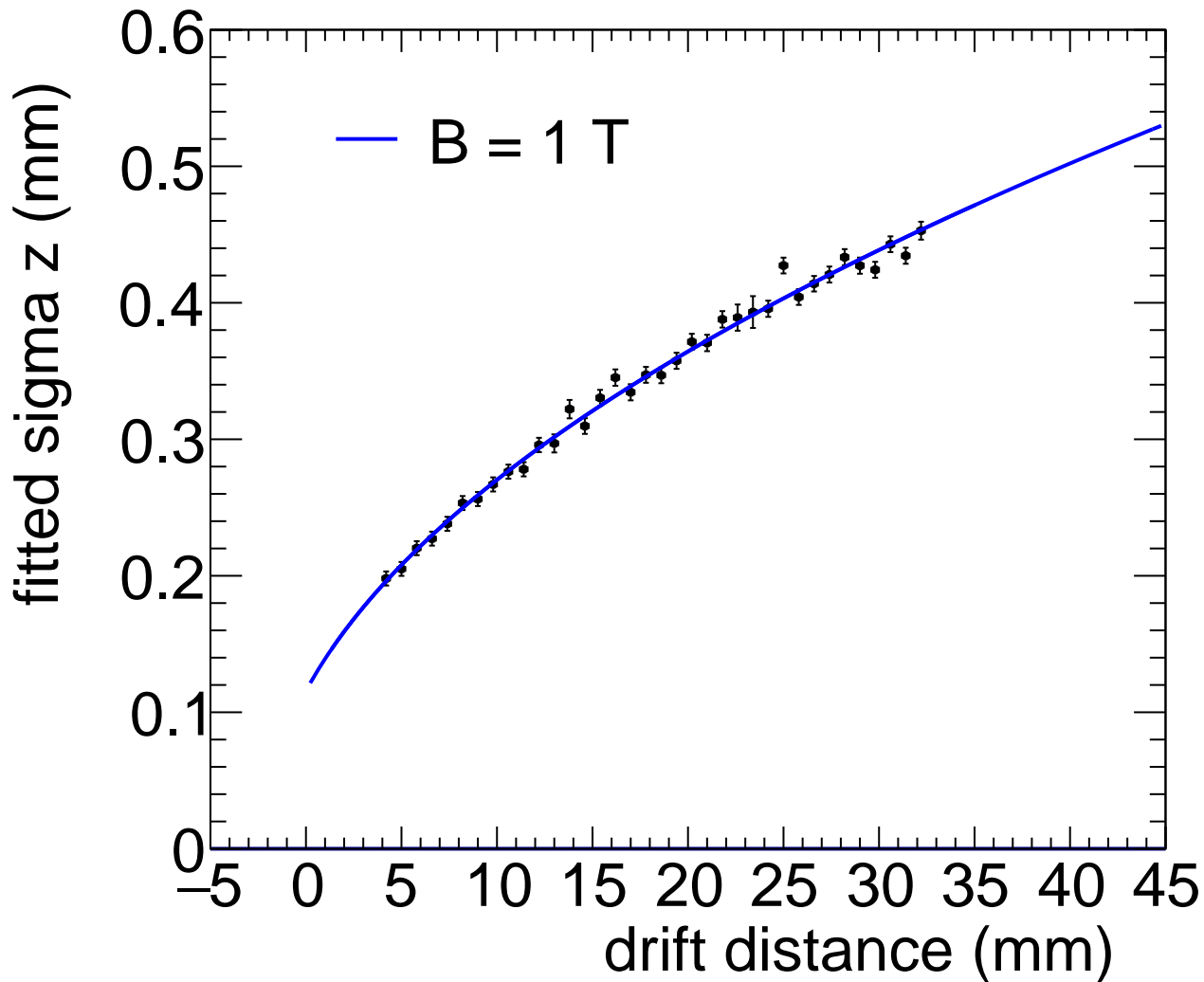
--Manuscript Draft--

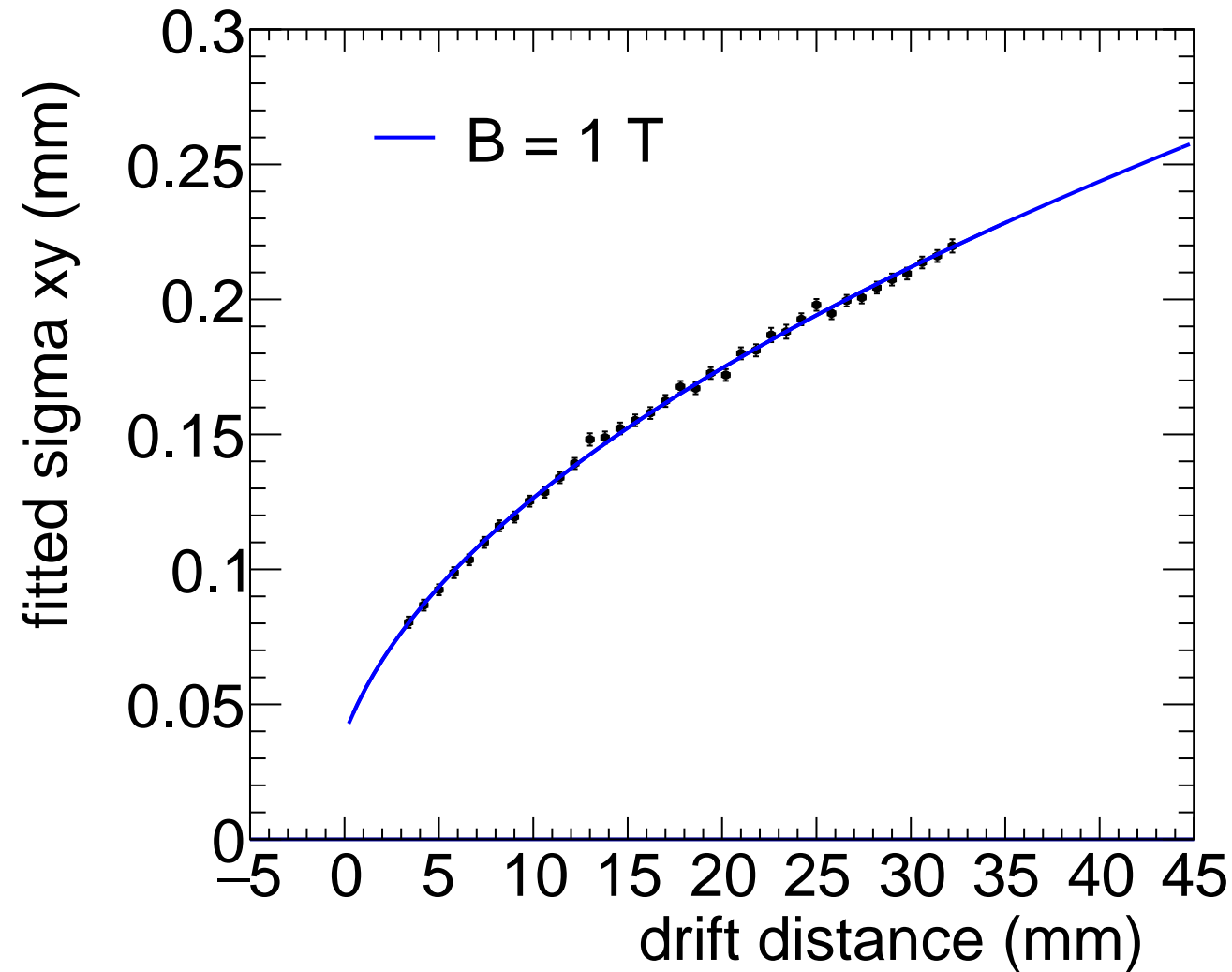
Manuscript Number:	NIMA-D-24-00682R1
Article Type:	Full length article
Section/Category:	High Energy and Nuclear Physics Detectors
Keywords:	Micromegas, gaseous pixel detector, micro-pattern gaseous detector, Timepix, GridPix, pixel time projection chamber
Corresponding Author:	Peter Kluit, Ph.D. Nationaal Instituut voor subatomaire fysica Amsterdam, Noord-Holland NETHERLANDS
First Author:	Peter Kluit, Ph.D.
Order of Authors:	Peter Kluit, Ph.D. Jochen Kaminsky, Dr other authors not listed here
Abstract:	<p>A Time Projection Chamber (TPC) module with 32 GridPix chips was constructed and the performance was measured using data taken in a testbeam at DESY in 2021. The GridPix chips each consist of a Timepix3 ASIC (TPX3) with an integrated amplification grid and have a high efficiency of about 85% to detect single ionisation electrons.</p> <p>In the testbeam setup, the module was placed in between two sets of Mimosas26 silicon detector planes that provided external high precision tracking and the whole detector setup was slid into the PCMAG magnet at DESY.</p> <p>The TPC could be operated reliably and used a 93.6/5.0/1.4 gas mixture (by volume) of Ar/iC4H10/CO2 with a small amount of oxygen and water vapour.</p> <p>The analysed data were taken at electron beam momenta of 5 and 6 GeV/c and at magnetic fields of 0 and 1 Tesla(T).</p> <p>The result for the transverse diffusion coefficient DT is $(287.2 \pm 0.5) \mu\text{m}/\sqrt{L}$ at $B = 0$ T and DT is $(120.3 \pm 0.5) \mu\text{m}/\sqrt{L}$ at $B = 1$ T.</p> <p>The longitudinal diffusion coefficient DL is measured to be $(251 \pm 14) \mu\text{m}/\sqrt{L}$ at $B = 0$ T and $(224 \pm 14) \mu\text{m}/\sqrt{L}$ at $B = 1$ T.</p> <p>Results for the tracking systematical uncertainties in xy (pixel plane) were measured to be smaller than $13 \mu\text{m}$ with and without magnetic field.</p> <p>The tracking systematical uncertainties in z (drift direction) were smaller than $15 \mu\text{m}$ ($B = 0$ T) and $20 \mu\text{m}$ ($B = 1$ T).</p>
Opposed Reviewers:	











Dear Reviewers

Thank you for the very careful reading of the manuscript. Your comments and questions have improved the quality of the manuscript significantly.

Here below the replies/[answers](#) to questions and remarks and [actions](#) in blue that were taken.

See you Peter Kluit

Reviewer #1: Please find minor line-by-line comments below:

50: readout -> read out

[Done](#)

50: SPIDR -> "SPIDR"

[Done:](#) replaced by (SPIDR)

61: In this paper,

[Done](#)

Table 1: was water content measured or determined from drift velocity measurements are described below?

[Answer:](#) We did not have a (e.g. sensor) measurement of the water content - only an estimate from the drift velocity measurements. NB: This point is mentioned in line 235.

232, 241: Please give values for the errors even if they are small.

[Done:](#) Dt 287.2 +- 0.5 (B=0) Dt 120.3 +- 0.5 (B=1)

279: Specify which hits were excluded - radius around pillars?

[Answer:](#) Only chips were excluded (detailed in lines 274-277).

The hits near the pillars were not rejected.

Hits near the edge in zone of 5 (10) pixels were removed.

As mentioned in lines 290-291.

289: Due to the presence of the dike,

[Done](#)

290: Therefore,

[Done](#)

312: Because of limited statistics,

Done

340: bias -> basis

Done

349: Telescope -> telescope

Done in many other places it was changed

363: place reference at end behind number to improve readability

Done: rephrased like: " for the T2K gas by \cite{Garfield},"

367: Time Projection Chamber -> TPC - already defined above

Done

Reviewer #2: The manuscript entitled "Towards a Pixel TPC part I: construction and test of a 32 chip GridPix detector" reports on the construction and first test beam results of a Time Projection Chamber (TPC) read out by 4 x 8 GridPix chips, 256 x 256 pixels each, and a maximum drift length of 40mm. Building upon previous detectors employing a single or four GridPix chips, the results presented in the manuscript are significantly new and important, a priori justifying publication in Nucl. Instr. Meth. Before doing so, however, a number of issues, related to the presentation and the analysis should be addressed.

Major comment a):

a) The manuscript is a bit sloppy about the use of the terms "resolution and residual". I insist that this is corrected. The resolution is related to the intrinsic performance of the detector. It does not include external uncertainties like the uncertainty of the reference track. The residual is the difference (measured - expected) hit positions for a single track/plane. The residual distribution is the distribution of residuals over many tracks. Being a distribution, it has a mean and a width. In this sense, e.g. Eq. (2) gives an expression for the width of the residual distribution, not the resolution. Figure 5 shows the measured width of the residual distribution (could be called residual width, if defined like that). Figure 7 shows the mean of the residual distribution (could be called residual mean, if defined). Similar examples can be found all along the manuscript. In addition, it is not explained in unambiguous terms, how exactly the residuals in xy and z are calculated. For every hit, one normally calculates the 3D-vector of the closest distance to the track. This vector projected onto the xy plane gives the residual in xy, its projection onto the z axis gives the residual in z. What value is used for the z coordinate (hit z position or track z position at DCA)? Please explain in the text. In Section 5.4, the authors talk about "tracking precision in the middle of the TPC". Please clearly define the term and explain how the numbers were obtained. Uncertainties (or rms values of the corresponding distributions) should be given for the numbers quoted.

Answer to Major Comment a)

Indeed, possible confusion about the residuals and the detector resolution should be avoided.

The definition of residual in xy and z is added. We use the standard definition: the distance of closest approach of the track in the xy plane is used and at that point the xy and z residuals are defined.

The text was corrected - in the following places - as proposed by the reviewer to avoid confusion.

Added at the beginning of section 5:

“The single electron hit resolutions in xy and z will be extracted from the residuals with respect to the fitted track. The track residual in xy is the closest point of the track in the xy plane to the hit at the center of the pixel. The residual in z is calculated at this point of closest approach. “

Rephrased subsection Hit resolutions in the pixel plane

“The residual of the hits in the pixel plane (xy) was measured as a function of the predicted drift position (z_{drift}).

The spread on the residual in xy for an ionisation electron is given by:

$\begin{equation}$

$$\sigma_{xy}^2 = \sigma_{\text{track}}^2 + \frac{d_{\text{pixel}}^2}{12} + D_T^2(z_{\text{drift}} - z_0),$$

$\text{\label{eq:sigmax}}$

$\end{equation}$

where σ_{track} is the uncertainty from the track prediction, d_{pixel} is the pixel pitch size, z_0 is the position of the grid, and D_T is the transverse diffusion coefficient. The last two terms correspond to the single electron detector resolution (squared).”

Caption of Figure 5 is also rephrased:

$\text{\caption{Measured spread on the residuals in the pixel plane (black points) fitted with equation \ref{eq:sigmax} (blue line).}}$

Rephrased subsection Hit resolutions in the drift plane:

The spread on the residuals in z of the ionisation electrons σ_z is given by:

$\begin{equation}$

$$\sigma_z^2 = \sigma_{\text{track}}^2 + \sigma_{z0}^2 + D_L^2(z_{\text{drift}} - z_0),$$

$\text{\label{eq:sigmaz}}$

$\end{equation}$

where σ_{track} is the expected track uncertainty, σ_{z0} the detector resolution at zero drift distance and D_L the longitudinal diffusion constant. The last two terms in the equation correspond to the single electron detector resolution (squared).”

Recall the definition of "the middle of the TPC"

The exact location of the "the middle of the TPC" was defined in line 177 as (at $y = 1436$ pixels). We added the location to the text in section 5.4 to remind the reader.

Major Comment b)

b) It is somewhat surprising that the statistical uncertainties on the measured diffusion coefficients are so small. What is the reduced χ^2 of the fits in Figs. 5 and 6? The authors say a few lines later that "the values of the diffusion coefficients depend on the humidity that was not precisely measured". In Line 192f, they write about "changes in the relative humidity of the gas volume due to leaks". Why does this not affect the extraction of D_T and D_L from the data? In addition, the statements in Line 234ff are hard to understand. Do the authors want to say that they obtained an estimate for the humidity from a comparison of the measured drift velocity with Magboltz, and that these humidity values were then used to obtain the $\pm 4\%$ quoted for the Magboltz "prediction" in Line 233? In any case, uncertainties (statistical or systematic or both) have to be attached to the measured values of the diffusion constants.

Answer to Comment b):

We agree that uncertainties for the transverse diffusion should be quoted in the paper (the uncertainties on the longitudinal diffusion were quoted).

The uncertainties are now quoted in the paper.

$Dt = 287.2 \pm 0.5$ (B=0) $Dt = 120.3 \pm 0.5$ (B=1)

The uncertainties are small because of the high statistics.

Q: What is the reduced χ^2 of the fits in Figs. 5 and 6?

Answer: The fit χ^2 for Figures 5 and 6 are:

Fig 5 left: 120.485 NDF 137 right: $\chi^2 = 18.9573$ NDF 35

Fig 6 left: 120.775 NDFz 121 right: $\chi^2 = 47.5922$ NDFz 34

Q: Why does this not affect the extraction of D_T and D_L from the data?

Answer The humidity will affect the MagBoltz predictions. The procedure to determine the humidity that was not measured is well described by the reviewer. The prediction from MagBoltz gets an uncertainty that is quoted.

Concerning systematic uncertainties. it was found out that there is a systematic uncertainty that affects the extraction of the longitudinal coefficient. The paper was corrected for this and a systematic error of $14 \mu\text{m}/\sqrt{\text{cm}}$ is quoted. Uncertainties (statistical or systematic or both) are attached to the measured values of the diffusion constants in the new version of the paper. Text is added to the paper to explain this.

Major Comment c)

c) It is somewhat difficult to reconcile the results for the resolution, the deformations and the efficiency, because it seems that they are based on different data sets or at least on different cuts applied to the data. For example, the track selection seems to be much stricter for the resolution studies in terms of fiducial cuts and amplitude (ToT) than for the efficiency. I understand that there may be reasons of

statistics, etc. to do so, but I still want to express my concern that in the end, for physics measurements, it is the combined performance for a given set of cuts that counts, not the best possible value for each single parameter, obtained under different conditions.

Answer to Comment c):

There are good reasons to apply selection and acceptance cuts. In particular for the studies that focus on the systematics in the TPC one has to apply strict cuts on matching cuts of the Telescope to the TPC to reject backgrounds.

We share the concern of the reviewer and the question "how does this extrapolate to a real experiment?" For TPC tracking in a real experiment the tracking efficiency is very close to one for the module because of the high single electron efficiency and the high number of electrons per crossed chip (See Fig 11: 124 B=0 and 89 B=1) and the high number of hits on the track that crosses the module of 8 chips ($8 \cdot 124$ and $8 \cdot 89$). Note that the number of electrons per crossed chip is after the hit selection (including a ToT cut).

Major Comment d)

d) The procedure leading to Figs. 8 and 10 is not understandable, at least not to this referee. The text in Lines 263 - 301 and in Lines 323 - 336 has to be completely rephrased in my opinion.

Answer to Comment d): the text is rephrased (see details below).

Q: "the module was regrouped in four 256x256 pixel planes put side by side on the horizontal axis",

Answer: To explain this better it was rephrased and a sentence was added

"the module was regrouped in $(4 \times 256) \times 256$ pixel planes put side by side on the horizontal axis, as shown in figure [\ref{fig:deformationsGroupedB0}](#). E.g. the selected chips from the upper left and bottom left quad detectors are combined into the 0-256 (x) and 0-256 (y) plane"

and

"Similarly, regrouping the module in $256 \times (4 \times 256)$ pixels put them side by side on the vertical axis,"

Q: "A bias in the mean residual..." => shouldn't this statement also be true for Figs. 7 and 9? If yes, it should be moved there.

Answer: Indeed we move the sentence up.

Q: "due to the presence of the dike pixels..." => dike pixels have not been defined

Answer: a comma was missing. "due to the presence of the dike, pixels"

Q: "the region near the edge of 5 pixels was removed"

Answer: "the region near the edge of the chip of 5 pixels"

Q: "a region of 10 pixels was removed"

Answer: "a region of 10 pixels near the edge of the chip was removed"

Q: what is the "expected statistical error"?

Answer: It is the expected uncertainty on the r.m.s. in the pixel (drift) plane for the regrouping and the available statistics. This is obtained by propagating the uncertainties. This is now added to the text.

Major Comment e)

e) Generally, the presentation towards the end of the manuscript (End of Section 5 and Section 6) seems to decline in quality with respect to the other Sections. I suggest that the authors have a closer look at these sections.

Answer: we followed up on the suggestions.

Q: In Section 5.4, no details are given on how the numbers are defined or extracted (see also comment a) above).

Answer: the uncertainties on the track parameters (position and angle) are propagated and the mean of these are given in this section. This explanation is added to the text.

Q: In Section 6, the difference between the number of hits (corresponding to number of ionization electrons) and the time over threshold (corresponding to charge after amplification in the Micromegas grid) should be made clear. In addition to the distributions of the number of hits, also the distributions of the ToT could be shown.

Answer: A sentence is added to explain that the ToT is related to the deposited charge. We will refer Fig 5.5 of the thesis of C Ligtenberg for a ToT distribution.

Q: The authors mention that the measured mean number of hits is in agreement with the prediction from ref. [13]. But given the Landau fluctuations of the number of ionization electrons and the large tail, wouldn't the most probable value be a better number for this comparison? Alternatively, one could show the predicted distribution along with the measured one.

Answer: From the MagBoltz calculations we have only the mean number for the T2K gas. We did not perform a full MC event-by-event simulation with Garfield/MagBoltz of the detector that would allow to extract the most probable value.

Additional comments:

Abstract:

- Line 19f: quoting the result for transverse and longitudinal diffusion coefficients without specifying the gas does not make sense.

Answer The uncertainties are quoted. Also a line is added to specify the gas.

- Line 20: remove "D_T is"

Done

- Line 22: the phrase "the diffusion measurements have negligible errors" is not valid. Every measurement must be accompanied by an estimate of the uncertainty!

Answer The line is removed and the results are quoted with uncertainties.

Introduction:

- Line 36: what clusters are meant here? Ionization clusters?

Answer: The primary clusters that each several ionization electrons.

- Line 43f: with an ENC of 70 e-, why is the threshold set to more than 7 sigma?

Answer To suppress the noise. The distribution has a non-gaussian tail. We don't want to flood our byte stream with noise hits. See also our previous publications.

- Line 45: be quantitative instead of claiming "high efficiency" I did not find the information on the number of pixels per TPX3 chip in the paper.

Answer: Indeed it is better to be quantitative. In the single chip paper an efficiency of about 80% is stated. In this paper we show a 85% single electron efficiency. We added in the introduction the 256x256 pixels.

We rephrased as "and a high efficiency of about 85% - demonstrated in this paper - to detect single ionisation electrons."

In the abstract we put: "high efficiency of about 85% ..."

- Line 50: "readout" => "read out"

Done (in many places)

Section 2:

- Line 72 and 89: "guard" => "guard electrode"

Done in more places we changed guard to guard electrode/strip etc.

- Line 86: "diameter"

Done

- Line 86: check use of "and"; what are the "guard strips"? Can they be indicated in Fig. 2?

Done "and" is removed. Guard strips are on the 4 sides of the module (in the quad plane).

Done: Fig 2 was updated: the different guard wires etc. are indicated

- Line 92: "two 50 um thick Kapton windows"

Done

Figure 1: should be enlarged

Done

- labels and a scale should be added

Not needed: Scales are in the text and in Figure 2

- "rendering"?

Done

- stick to either "32-GridPix module" instead of "8-quad module" throughout the text

Done

Figure 2: add labels, e.g. for guard wires, guard strips, guard electrodes, pillars for field wires, etc.

Done: We added color coding and explanation in the caption

Section 3:

- Line 114: "At DESY, the Mimosa26 silicon..." (add comma and remove parentheses)

Done

- Line 124: "parameters"

Done everywhere parametres->parameters

- Line 125: add "and" before "oxygen"

Done

- Line 134: "systems"

Done

- Line 137: "of" => "with respect to"

Done (rephrased)

Figure 3: is this a top or side view?

Answer Side view:

Captions reads as "Photo of the detector setup - side view - at the centre of the PCMAG magnet (the circular contour) . The Mimosa26 planes M0 and M3 are indicated in red as well as the beam direction (yellow)."

The main text now has "The stage positions the TPC module with respect to the beam and the Mimosa26 planes can be adjusted."

Table 1:

- is the number of runs important?

Answer: Not crucial, but this is important if somebody wants to redo the analysis (Open Data Acces)

- are the beam momenta relevant? (see also corresponding comment below)

Answer: Yes, the multiple scattering is a bit different and the electron/trigger rates are different.

Section 4:

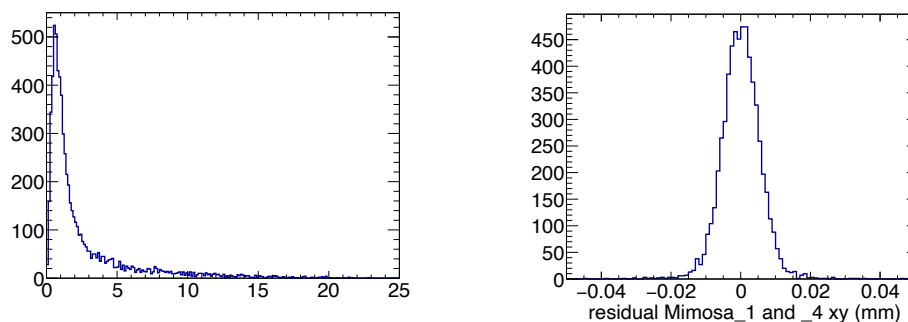
- Line 155: check language in "Telescope tracks were selected with at least 5 out of 6 planes on the track" => "Telescope tracks were required to have hits in at least 5 out of the 6 planes"

Done

- Line 156: why is the track χ^2 cut so large? What is the distribution of the reduced χ^2 ?

Answer: The value was chosen to keep a high tracking and silicon plane "on track" efficiency.

Plots for the χ^2/ndof and the residuals in the M1 plane



- Line 176: with respect to what has the acceptance window for GridPix hits been defined?

Answer: it reflects the size of the quartz window

- Line 177: "was" => "were"

Done

- Line 179: check language in "quadratic track B=1 T model"

Done

- Line 180: give values for the "expected uncertainties". How were they obtained?

Answer: A sentence was added to clarify this "The expected uncertainties were derived using the parametrisations discussed in section [\ref{sec:hitResolution}](#)."

- Line 181f: the phrase "outlier removal at respectively 10, 5 and 2.5 sigma level" is hard to understand, please rephrase. What sigma do you refer to here?

Answer: Here sigma means the expected uncertainty on the hit. Text change to "The fit was iterated three times to reject outlier hits at respectively 10, 5 and 2.5 sigma."

- Line 183: why do only 25% of all hits lie on the track? Figure 4 looks much cleaner. Please explain.

Answer: the text says "More than 25%". In most (clean) cases all the hits end up on the track.

- Line 185: what orientation does the "plane in the middle of the TPC" have?

Answer: $y = \text{constant}$. So x and z any value: so orthogonal to the main beam direction.

- Line 199: add "from" before "run"

Done

Figure 4: - red and blue lines are hard to distinguish- green points are hardly visible

Answer: not easy to make this better without spoiling the overall picture. In the electronic version one can zoom and see it.

- "driftplane => "drift plane"

Done

Section 5:

- Line 208: "Secondly" would require a "firstly" before

Done Added Firstly,

- Line 220: "staying 20 pixels away from the chips edges" => are all 4 chips edges meant here?

Answer: Only the chip edges in local x (orthogonal to the beam). Text is now "staying 20 pixels away in local x from the chip edges"

- Line 221: see above comment on "resolution"

Answer already discussed under Major Comment a)

- Eq. (2): give a reference, e.g. [Yonamine et al., JINST 9 (2014) C03002]

Answer: We think it is not needed to cite a reference: one can also find the expression in our previous papers.

- Line 228f: "sensors", "windows"

Done

- Line 244f: "resolution ... in the drift plane" => should be "residual width in z direction"? The expression "drift plane" has not been defined.

Answer: this has been rephrased. The z direction is the drift direction.

- Line 249: why is the ToT cut chosen for the z residuals so much higher than the one applied for the xy residuals (0.6 μ s vs 0.15 μ s)? How does this affect the efficiency?

Answer: The time slewing - that depends on the ToT - has an important impact on the resolution of the detector. This has been discussed in our single chip paper ref 1. There we used a ToT cut at 0.6 μ s. The efficiency of the cut is about 50%. NB For TPC tracking we use of course all hits with ToT > 0.15 μ s.

- Line 257: what do the authors conclude from the discrepancy between the measured value of D_L and Magboltz? Is Magboltz data wrong, or are there systematic effects that were not taken into account?

Answer we followed up on the longitudinal Diffusion this point and found a systematic uncertainty that was over looked - as discussed above. The results are in better agreement now.

- Line 274f: it would greatly facilitate reading if the chip numbers quoted in the text were visible in Figs. 7 and 9, without having to go back a few pages to Fig. 2.

Answer: The reader can find the information and the text also explains where the chips are ("corner chips").

- Line 302: "electrons will drift mainly along the magnetic field lines" seems not entirely correct. What is the value of $\omega\tau$? I suggest to remove the sentence, as it is not needed.

Answer: $\omega\tau$ is about 4.5 and. So the electrons drift mainly according to the B field lines.

- Line 312: mention that these are now biased residuals, in contrast to the ones for $B=0T$, where the external track was used as reference

Done

Figures 7, 9:- add labels and units for z axis

Answer: We changed the caption "Mean residuals (color coded in mm) ...

- is the binning really 8×16 pixels? Zooming in, it seems that there is an equal number of bins in x and y for each chip, which would imply an 8×8 binning.

Answer: Thanks for spotting this. The bin size is indeed 16×16 in xy and z. This is now corrected in the paper.

Figures 8,10:- add labels and units for z axis

Answer: see above: we changed the caption "Mean residuals (color coded in mm) ...

- what is the "regrouped expected hit position"?

Answer: "the expected hit position" (in the plane). Text changed.

Section 6:

- Line 350f: check language in "the $B=0T$ analysis selects the" => "For the analysis of the data with $B=0T$, the chips ... were selected" or similar?

Done

- Line 352: why were chips 12, 13, 20, and 21 excluded for the $B=0T$ analysis? For a proper comparison of $B=0$ and $1T$ data, wouldn't it be advisable to use the same data set?

Answer For $B=1$ chips 12, 13, 20, and 21 could be included because of the different Beam angle in the $B=1$ data set that allowed a larger acceptance. One could remove these chips (12,13,20,21) for "consistency" but that would decrease the statistics.

- Line 362: typo in "possibility"

Done

Figure 11:

- typo in "per per" - check language in caption

Done

Section 7:

- the authors emphasize here again that data were taken at two different beam momenta, but throughout the analysis in the previous sections, no mention is made, which beam momentum the data correspond to. Have both momenta been used, e.g. also for Section 6? Probably the authors should state for each Section, which beam momenta were used

Answer: The data correspond to beam momenta of 5 and 6 GeV in all sections. In section 6 too (this has been corrected).

- Line 380f: this statement does not make much sense, unless an explicit public link to the data is given

Answer: One can contact LCTPC/DESY or the author for the links (note that Grid links do change).

Language and format:

- put symbols for physical quantities in italics: B , x , y , etc.

- do not put units in italics, e.g. GeV, cm

- use mathematical symbols where applicable, e.g. " \times " instead of "x"

- use SI units where applicable, e.g. there is no need to define T as Tesla when talking about magnetic field strength

- check use of hyphens (missing very often, especially in compound modifiers like "32-chip module", "high-precision tracking",...)

- references: should be in square brackets, not in parentheses; use [1,2] instead of (1), (2).

- format tables 1 and 2 for better readability

- slided => slid

- avoid use of jargon, e.g. "quads", "guard", etc.

- avoid unphysical statements like "great precision", "high efficiency", ...


- check use of commas

All Done



Click here to access/download
LaTeX Source Files
quadbox_v0.pdf






Click here to access/download
LaTeX Source Files
eventDisplay_DESY.pdf

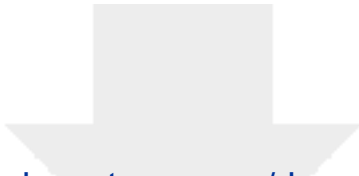




Click here to access/download

LaTeX Source Files
HitsChip6981-88.pdf

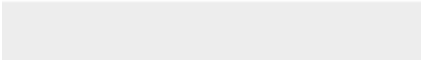


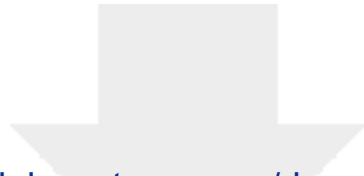


Click here to access/download

LaTeX Source Files

HitsChip6909-16-17-34-35.pdf

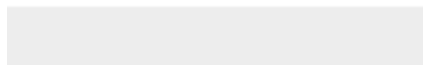


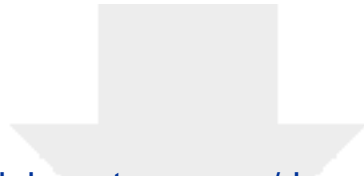


Click here to access/download

LaTeX Source Files

DeformTeleCorMapRun6909-16-17-34-35.pdf

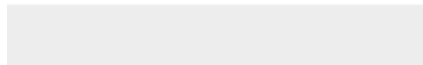
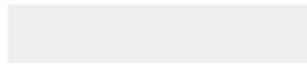


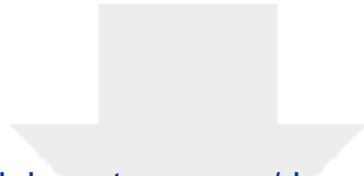


[Click here to access/download](#)

LaTeX Source Files

[DeformTCorRowMapRun6909-16-17-34-35.pdf](#)





Click here to access/download

LaTeX Source Files

DeformCorRowMapRun6981-88.pdf

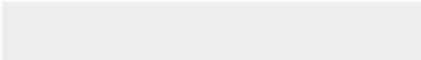




Click here to access/download

LaTeX Source Files

DeformCorMapRun6981-88.pdf





Click here to access/download

LaTeX Source Files
DESYsetup_v1.jpg



Declaration of interests

The authors declare that they have no known competing financial interests or personal relationships that could have appeared to influence the work reported in this paper.

The authors declare the following financial interests/personal relationships which may be considered as potential competing interests:

1 Towards a Pixel TPC part I: construction and test of a
2 32-chip GridPix detector

3 M. van Beuzekom^a, Y. Bilevych^b, K. Desch^b, S. van Doesburg^a,
4 H. van der Graaf^a, F. Hartjes^a, J. Kaminski^b, P.M. Kluit^a,
5 N. van der Kolk^a, C. Ligtenberg^a, G. Raven^a, J. Timmermans^a

6 ^a*Nikhef, Science Park 105, 1098 XG Amsterdam, The Netherlands*

7 ^b*Physikalisches Institut, University of Bonn, Nussallee 12, 53115 Bonn,*
8 *Germany*

9 **Abstract**

10 A Time Projection Chamber (TPC) module with 32 GridPix chips was con-
11 structed and the performance was measured using data taken in a testbeam
12 at DESY in 2021. The GridPix chips each consist of a Timepix3 ASIC
13 (TPX3) with an integrated amplification grid and have a high efficiency of
14 about 85% to detect single ionisation electrons. In the testbeam setup, the
15 module was placed in between two sets of Mimosas26 silicon detector planes
16 that provided external high precision tracking and the whole detector setup
17 was slid into the PCMAG magnet at DESY. The TPC could be operated
18 reliably and used a 93.6/5.0/1.4 gas mixture (by volume) of Ar/iC₄H₁₀/CO₂
19 with a small amount of oxygen and water vapour. The analysed data were
20 taken at electron beam momenta of 5 and 6 GeV/c and at magnetic fields of
21 0 and 1 T.

22 The result for the transverse diffusion coefficient D_T is (287.2 ± 0.5)
23 $\mu\text{m}/\sqrt{\text{cm}}$ at $B = 0$ T and D_T $(120.3 \pm 0.5) \mu\text{m}/\sqrt{\text{cm}}$ at $B = 1$ T. The
24 longitudinal diffusion coefficient D_L is measured to be $(251 \pm 14) \mu\text{m}/\sqrt{\text{cm}}$

*Corresponding author, Telephone: +31 20 592 2000
Preprint submitted to Nuclear Instruments and Methods A
Email address: s01@nikhef.nl (P.M. Kluit)

25 at $B = 0$ T and $(224 \pm 14) \mu\text{m}/\sqrt{\text{cm}}$ at $B = 1$ T. Results for the tracking
26 systematical uncertainties in xy (pixel plane) were measured to be smaller
27 than $13 \mu\text{m}$ with and without magnetic field. The tracking systematical
28 uncertainties in z (drift direction) were smaller than $15 \mu\text{m}$ ($B = 0$ T) and
29 $20 \mu\text{m}$ ($B = 1$ T).

30 *Keywords:*

31 Micromegas, gaseous pixel detector, micro-pattern gaseous detector,
32 Timepix, GridPix, pixel time projection chamber

33 1. Introduction

34 Earlier publications on a single chip [1] and four chip (quad) GridPix de-
35 tectors [2] showed the potential of the GridPix technology and the large range
36 of applications for these devices [3]. In particular, it was demonstrated that
37 single ionisation electrons can be detected with high efficiency and accuracy,
38 allowing excellent 3D track position measurements and particle identification
39 based on the number of electrons and clusters.

40 As a next step towards a Pixel Time Projection Chamber for a future
41 collider experiment [4], [5], a module consisting of 32 GridPix chips based on
42 the TPX3 chip was constructed.

43 A GridPix detector consists of a CMOS pixel TPX3 chip [6] with inte-
44 grated amplification grid added by photo-lithographic - Micro-electromechanical
45 Systems (MEMS) - post-processing techniques. The TPX3 chip can be op-
46 erated with a low threshold of $515 e^-$, and has a low equivalent noise charge
47 of about $70 e^-$. The GridPix single chip and quad detectors have a very
48 fine granularity of $55 \times 55 \mu\text{m}^2$ with 256×256 pixels per chip. The device has

49 a high efficiency of about 85% - discussed in this paper - to detect single
50 ionisation electrons.

51 Based on the experience gained with these detectors a 32 GridPix detector
52 module - consisting of 8 quad detectors - was built. A drift box defining the
53 electric field and gas envelop was constructed. A read out system for up to
54 128 chips with 4 multiplexers read out by one Speedy Pixel Detector Readout
55 (SPIDR) board [7] [8] was designed. After a series of tests using the laser
56 setup [9] and cosmics in the laboratory at Nikhef, the detector was taken to
57 DESY for a two week testbeam campaign.

58 At DESY, the 32-chip detector was placed in between two sets of Mi-
59 mosa26 silicon detector planes and mounted on a movable stage. The whole
60 detector setup was slid into the centre of the PCMAG magnet at DESY. A
61 beam trigger was provided by scintillator counters. The data reported here
62 were taken at different stage positions and electron beam momenta of 5 and
63 6 GeV/c and at magnetic fields of 0 and 1 T. The performance of the 32
64 GridPix detector module was measured using these data sets.

65 In this paper, part I of the results will be presented with the main focus
66 on the detector spatial resolution and tracking performance. A second follow
67 up paper will discuss the dE/dx (or dN/dx) and other results.

68 **2. The 32-GridPix detector module**

69 A 32 GridPix detector module was built using the quad detector module
70 [2] as a basic building block. The quad module consists of four GridPix chips
71 and is optimised for a high fraction of sensitive area of 68.9%. The external
72 dimensions are 39.60 mm \times 28.38 mm. The four chips which are mounted

73 on a cooled base plate (COCA), are connected with wire bonds to a common
74 central 6 mm wide PCB. A 10 mm wide guard electrode is placed over the
75 wire bonds 1.1 mm above the aluminium grids, in order to prevent field
76 distortions of the electric drift field. The guard electrode is the main inactive
77 area, and its dimensions are set by the space required for the wire bonds.
78 On the back side of the quad module, the PCB is connected to a low voltage
79 regulator. The aluminium grids of the GridPix detectors are connected by
80 80 μm insulated copper wires to a high voltage (HV) filtering board. The
81 quad module consumes about 8 W of power of which 2 W is used in the LV
82 regulator.

83 Eight quad modules were embedded in a box, resulting in a GridPix
84 detector module with a total of 32 chips. A schematic 3-dimensional drawing
85 of the detector is shown in Figure 1. A schematic drawing of the quad
86 detectors in the module is shown in Figure 2, where also the beam direction
87 is indicated.

88 The internal dimensions of the box are 79 mm along the x -axis, 192 mm
89 along the y -axis, and 53 mm along the z -axis (drift direction), and it has a
90 maximum drift length (distance between cathode and read out anode) of 40
91 mm. The drift field is shaped by a series of parallel CuBe field wires of 75
92 μm diameter with a wire pitch of 2 mm. Guard strips are located on all of
93 the four sides of the active area. In addition, six guard wires - shown with
94 dashed lines (one colored red) in Figure 2 - are suspended over the boundaries
95 of the chips, to minimise distortions of the electric drift field. The wires are
96 located at a distance of 1.15 mm from the grid planes, and their potential is
97 set to the drift potential at this drift distance. The box has two 50 μm thick

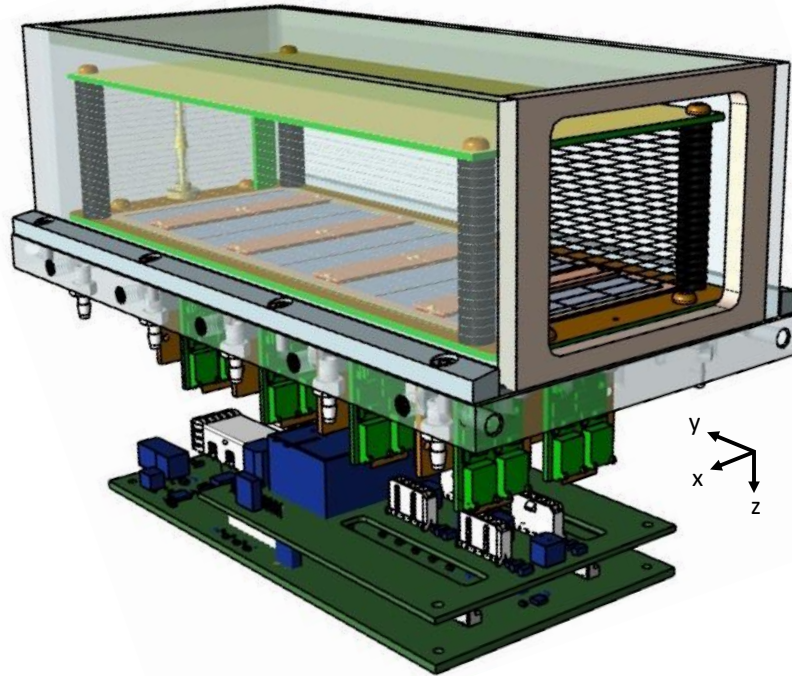


Figure 1: Schematic 3-dimensional rendering of the 32-GridPix module detector for illustration purposes.

98 Kapton windows to allow the beam to pass with minimal multiple scattering.
99 The gas volume of 780 ml is continuously flushed at a rate of ~ 50 ml/min
100 (about 4 volumes/hour) with premixed T2K TPC gas. This gas is a mixture
101 consisting of 95% Ar, 3% CF_4 , and 2% iC_4H_{10} suitable for large TPCs because
102 of the low transverse diffusion in a magnetic field and the high drift velocity.
103 The data acquisition system of the quad module was adopted to allow for
104 reading out multiple quad detectors. A multiplexer card was developed that
105 handles four quad detectors or 16 chips and combines the TPX3 data into
106 one data stream. For the 32 GridPix module two multiplexers are connected
107 to a SPIDR board that controls the chips and read out process. The read

108 out speed per chip is 160 Mbps and for the multiplexer 2.56 Gbps this cor-
 109 responds to a maximum rate of 21 MHits/s. For each pixel the precise Time
 110 of Arrival (ToA) using a 640 MHz TDC and the time over threshold (ToT)
 111 are measured.

112 3. Experimental setup

113 In preparation of the two weeks DESY testbeam campaign, a support
 114 frame was designed to move the 32-chip GridPix detector module in the
 115 plane perpendicular to the beam by a remotely controlled stage such that
 116 the whole detector volume could be probed. The module was mounted upside
 117 down with respect to Figure 1 to allow access to the electronics from above.

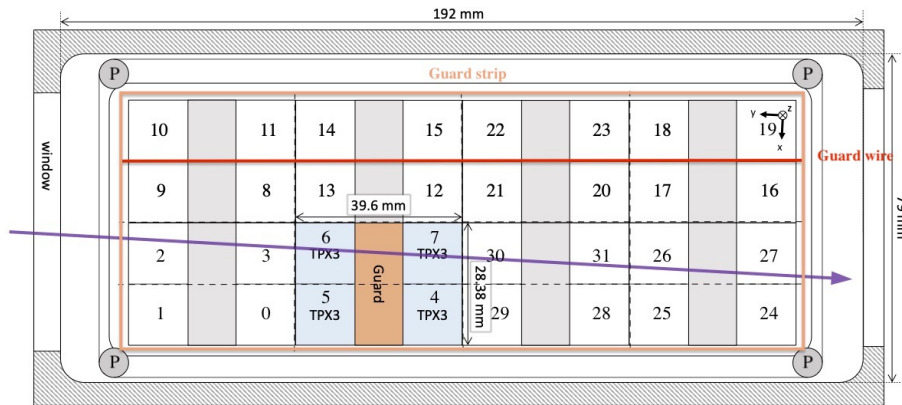


Figure 2: Schematic drawing of the 32-GridPix module detector with one example quad as viewed from the top of the quad detectors. The chips are numbered and the beam direction is shown in purple. A guard electrode of a quad detector is shown in orange. The four surrounding guard strips are shown -not to scale- in orange. Six guard wires - are shown with dashed lines (one colored red) and the pillars of the drift box are shown as circles with a P in the centre.

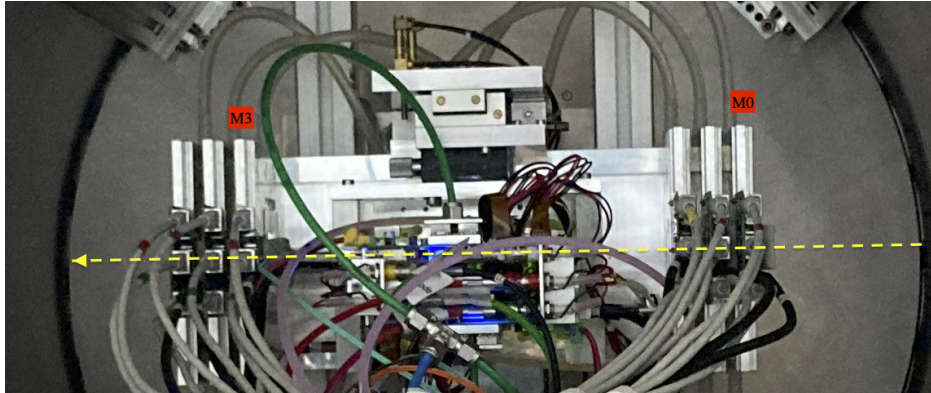


Figure 3: Photo of the detector setup - side view - at the centre of the PCMAG magnet (the circular contour). The Mimosa26 planes M0 and M3 are indicated in red as well as the beam direction (yellow).

118 The support frame also held three Mimosa26 silicon detector planes [10] -
119 with an active area of $(21.2 \text{ mm} \times 10.6 \text{ mm})$ - placed in front of the detector
120 and three Mimosa26 planes behind the detector. At DESY, the Mimosa26
121 silicon detector planes were provided by the testbeam coordinators. The
122 whole detector setup was slid towards the centre of the PCMAG magnet
123 at the DESY II testbeam facility [10]. A beam trigger was provided by a
124 double scintillator counter coincidence. The data were taken at different
125 stage positions to cover the whole sensitive TPC volume. Runs with electron
126 beam momenta of 5 and 6 GeV/c and at magnetic fields of 0 and 1 T were
127 analysed.

128 A photograph of the detector setup in the PCMAG magnet is shown in
129 Figure 3. The stage positions of the TPC module with respect to the beam
130 and the Mimosa26 planes can be adjusted.

131 The experimental and environmental parameters such as temperature,

132 pressure, gas flow and oxygen content were measured and logged by a Win-
 133 dows operated slow control system. The experimental parameters are sum-
 134 marised in Table 1. The chips were cooled by circulating Glycol through
 135 the cooling channels in the module carrier plate. The cooling blocks of the
 136 multiplexers were further cooled by blowing pressurised air on them.

Table 1: Overview of the experimental parameters. The ranges indicate the variation over the data taking period

Number of analysed runs at $B=0$ (1) T	6 (8)
Run duration	10-90 minutes
Number of triggers per run	3-100 k
E_{drift}	280 V/cm
V_{grid}	340 V
Threshold	550 e ⁻
Gas temperature	303.3-306.6 K
Pressure	1011 – 1023 mbar
Oxygen concentration	240 - 620 ppm
Water vapour concentration	2000 - 7000 ppm

137 The data was produced in four main data streams: one stream produced
 138 by the Mimosa26 telescope, two data streams by the two Timepix multiplex-
 139 ers and one trigger stream. The double scintillator coincidence provided a
 140 trigger signal to the Trigger Logic Unit (TLU) [11] that sends a signal to the
 141 telescope read out and the trigger SPIDR. The data acquisition systems of
 142 the telescope and trigger SPIDR injected a time stamp into their respective
 143 data streams. Hits from the Mimosa26 planes were collected with a sliding
 144 window of $-115 \mu\text{s}$ to $230 \mu\text{s}$ around the trigger time. The data acquisition

145 of the multiplexer and the trigger SPIDR were synchronised at the start of
146 the run. By comparing the time stamps in these streams, telescope tracks
147 and TPC tracks could be matched. Unfortunately, the SPIDR trigger had
148 - due to a cabling mistake at the output of the TLU - a common 25 ns flat
149 time jitter.

150 After a short data taking period one of the chips (nr 11) developed a
151 short circuit and the HV on the grid of the chip was disconnected. After the
152 testbeam data taking period the module was repaired in the clean room in
153 Bonn.

154 4. Analysis

155 4.1. Telescope track reconstruction procedure

156 The data of the telescope is decoded and analysed using the Corryvreckan
157 software package [12]. The track model used for fitting was the General
158 Broken Lines (GBL) software [14]. The code was extended and optimised to
159 fit curved broken lines for the data with magnetic field. The telescope planes
160 were iteratively aligned using the standard alignment software provided by
161 the package. The single point Mimosas26 resolution is $4 \mu\text{m}$ in x and $6 \mu\text{m}$
162 in z (drift direction) [10].

163 Telescope tracks were selected were required to have hits in at least 5 out
164 of the 6 planes and a total χ^2 of better than 25 per degree of freedom. The
165 uncertainties on the telescope track prediction in the middle of the GridPix
166 detector module are dominated by multiple scattering. The amount of mul-
167 tiple scattering was estimated by comparing the predictions from the two
168 telescope arms for 6 GeV/c tracks at $B = 0$ T. The expected uncertainty in

169 x and z is $26 \mu\text{m}$ on average.

170 4.2. TPC Track reconstruction procedure

171 GridPx hits are selected requiring a minimum time over threshold ToT
172 of $0.15 \mu\text{s}$. The drift time is defined as the measured time of arrival minus
173 the trigger time recorded in the trigger SPIDR data stream minus a fixed t_0
174 (the drift time at zero drift). The drift time was corrected for time walk [2]
175 using the measured time over threshold (ToT in units of μs) and the formula
176 (1):

$$\delta t = \frac{18.6(ns \mu s)}{\text{ToT} + 0.1577(\mu s)}. \quad (1)$$

177 Furthermore, small time shift corrections - with an odd-even and a $16 \times$ pixels
178 structure - coming from the TPX3 clock distribution were extracted from the
179 data and applied.

180 The z drift coordinate was calculated as the product of the drift time
181 and the drift velocity. This implies that $z_{\text{drift}} = -z$ as defined in Figure 1.
182 GridPix hits outside an acceptance window of 30 mm wide in x and 15 mm
183 wide in z were not used in the track finding and reconstruction. Based on
184 a Hough transform an estimate of the TPC track position and angles in the
185 middle of the module (at $y = 1436$ pixels) were obtained. This estimate was
186 used to collect the hits around the TPC track and fit the track parameters.
187 For this fit a linear (for $B = 0 \text{ T}$ data) or a quadratic track (for $B = 1 \text{ T}$ data)
188 model was used. In the fit, the expected uncertainties per hit σ_{xy} and σ_z were
189 used. The expected uncertainties were derived using the parametrisations
190 discussed in section 5. The fit was iterated three times to reject outlier hits

Table 2: Table with track/event selection cuts

Track/Event Selection

$$|x_{\text{TPC}} - x_{\text{telescope}}| < 0.3 \text{ mm}$$

$$|z_{\text{TPC}} - z_{\text{telescope}}| < 2 \text{ mm}$$

$$|dx/dy_{\text{TPC}} - dx/dy_{\text{telescope}}| < 4 \text{ mrad}$$

$$|dz/dy_{\text{TPC}} - dz/dy_{\text{telescope}}| < 2 \text{ mrad}$$

191 at respectively 10, 5 and 2.5 sigma. A TPC track was required to have a
192 least 100 hits in each multiplexer. At least 25% of the total number of hits
193 should be on track and the χ^2 per degree of freedom had to be less than 3 in
194 xy and zy . All track parameters were expressed at a plane in the middle of
195 the TPC module.

196 The calibration and alignment of the detector was done using high quality
197 tracks for which the track selections are summarised in table 2.

198 The drift velocity was calibrated per run by fitting a linear function to
199 the z (predicted from the telescope track at the measured TPC hit position)
200 versus the measured drift time in the TPC. For the $B = 0$ T runs it varies
201 between 61.6 and 63.0 $\mu\text{m}/\text{ns}$. For the $B = 1$ T runs it is between 57.2 and
202 59.1 $\mu\text{m}/\text{ns}$. The variation comes mainly from the changes in the relative
203 humidity of the gas volume due to small leaks.

204 The individual TPX3 chips were iteratively aligned fitting a shift in x
205 (z *drift*) and two slopes $dx(z \text{ drift})/drow(\text{column})$. The alignment was
206 done per run, because the detector was moved in x and/or z for each run.
207 The fitted slopes were also corrected for small shifts and rotations (3D) in
208 the nominal chip position.

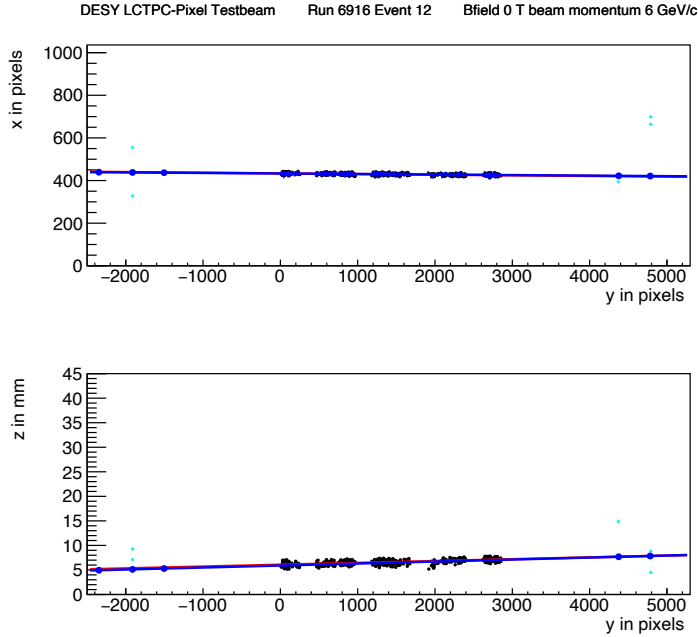


Figure 4: An event display for run 6916 without B field, with in total 1293 TPC hits (black dots) in the precision plane (x, y) and drift plane $(z \text{ drift}, y)$. The fitted TPC track (red line) with 1130 hits on track and the telescope track (blue line) with 5 Mimosa26 planes (blue hits) on track are shown. In green the off track Mimosa26 hits are shown.

209 An example event from run 6916 without B field with a TPC and a
 210 telescope track is shown in Figure 4. The TPC is located between $y = 0$ and
 211 2872 pixels. Three Mimosa26 planes are located at $y < -1000$ and three at
 212 $y > 4000$ pixels.

213 5. Hit resolutions

214 The track residual in xy is the closest point of the the hit at the center
 215 of the pixel to track in the xy plane. The residual in z is calculated at this
 216 point of closest approach. The single electron hit resolutions in xy and z will

217 be extracted from the track residuals. In order to study the single electron
 218 resolution for the data with and without magnetic field, additional selections
 219 on the telescope and TPC tracks were applied. Firstly, due to the trigger
 220 time jitter of 25 ns (corresponding to 1.5 mm drift), the prediction of the
 221 telescope track in z must be used as the reference for z . Secondly, the z hits
 222 of the TPC track were fitted to correct for the common time shift and the
 223 z residuals were calculated with respect to the fitted TPC track. In the xy
 224 plane the residuals of TPC hits with respect to the telescope track were used
 225 to extract the single electron resolution in xy . For the resolution studies,
 226 runs at three different z stage positions of the TPC were selected where the
 227 beam gave hits in the central chips. The data of 14 central chips (9, 12, 21,
 228 20, 17, 16, 2, 3, 6, 7, 30, 31, 26 and 27) were used. Two chips (8 and 13)
 229 were left out because of the E field deformations caused by the short circuit
 230 in chip 11.

231 5.1. Hit resolutions in the pixel plane

232 The residual of the hits in the pixel plane (xy) was measured as a function
 233 of the predicted drift position (z_{drift}). Tracks were selected that crossed the
 234 fiducial region defined by the central core of the beam. Hits were removed
 235 in a region of 20 pixels near the chip edges in x . The spread on the residual
 236 in xy for an ionisation electron is given by:

$$\sigma_{xy}^2 = \sigma_{\text{track}}^2 + \frac{d_{\text{pixel}}^2}{12} + D_T^2(z_{\text{drift}} - z_0), \quad (2)$$

237 where σ_{track} is the uncertainty from the track prediction, d_{pixel} is the pixel
 238 pitch size, z_0 is the position of the grid, and D_T is the transverse diffusion
 239 coefficient. The last two terms correspond to the single electron detector

240 resolution (squared). The resolution at zero drift distance $d_{\text{pixel}}/\sqrt{12}$ was
 241 fixed to $15.9 \mu\text{m}$ and σ_{track} to $30 \mu\text{m}$ for $B = 0 \text{ T}$ and $42 \mu\text{m}$ for $B =$
 242 1 T data. The uncertainty on the track prediction was measured and is
 243 larger than the Mimosa plane resolution because of multiple scattering in
 244 the sensors and in the entrance and exit windows.

245 The expression (2) - leaving z_0 and D_T as free parameters - is fitted
 246 to the $B = 0 \text{ T}$ data shown in Figure 5. The fit gives a transverse diffusion
 247 coefficient D_T of $(287.2 \pm 0.5) \mu\text{m}/\sqrt{\text{cm}}$. The measured value is in agreement
 248 with the value of $287 \mu\text{m}/\sqrt{\text{cm}} \pm 4\%$ predicted by the gas simulation software
 249 Magboltz 11.9 [15]. The values of the diffusion coefficients depend on the
 250 humidity that was not precisely measured during the testbeam. The humidity
 251 strongly affects the drift velocity. Therefore the drift velocity prediction from
 252 Magboltz was used to determine the water content per run and predictions
 253 for the diffusion coefficients could be obtained.

254 A fit to the $B = 1 \text{ T}$ data, also shown in Figure 5, gives a transverse
 255 diffusion coefficient D_T of $(120.3 \pm 0.5) \mu\text{m}/\sqrt{\text{cm}}$. The measured value is in
 256 agreement with the value of $119 \mu\text{m}/\sqrt{\text{cm}} \pm 2\%$ predicted by Magboltz.

257 5.2. Hit resolution in the drift plane

258 The spread on the residuals in z of the ionisation electrons σ_z is given by:

$$\sigma_z^2 = \sigma_{\text{track}}^2 + \sigma_{z_0}^2 + D_L^2(z_{\text{drift}} - z_0), \quad (3)$$

259 where σ_{track} is the expected track uncertainty, σ_{z_0} the detector resolution at
 260 zero drift distance and D_L the longitudinal diffusion constant. The last two
 261 terms in the equation correspond to the single electron detector resolution
 262 (squared). Only tracks crossing the fiducial region - defined by the central

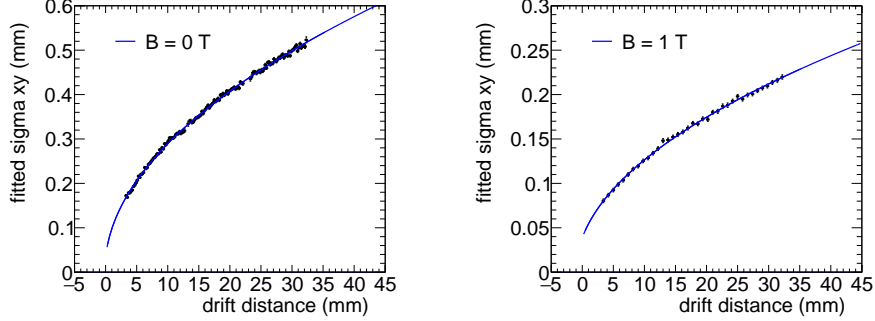


Figure 5: Measured spread on the residuals in the pixel plane (black points) fitted with equation (2) (blue line).

263 core of the beam - were accepted and hits with a ToT value above $0.6 \mu\text{s}$
 264 were selected. Because of the time jitter, the fitted TPC track is used for the
 265 drift residuals. For z_{drift} the telescope prediction at the hit was used. The
 266 expected uncertainty on TPC track prediction is propagated and amounts to
 267 $50 \mu\text{m}$ at $z = z_0$. The systematic uncertainty on σ_{track} is estimated to
 268 be $25 \mu\text{m}$.

269 The expression (3) - leaving σ_{z_0} and D_L as free parameters - is fitted
 270 to the $B = 0 \text{ T}$ data shown in Figure 6. The value of z_0 was fixed to the
 271 result of the fit in the xy plane. The value of σ_{z_0} was measured to be 129
 272 μm . The longitudinal diffusion coefficient D_L was determined to be $(251$
 273 $\pm 1 \text{ (stat)} \pm 14 \text{ (sys)}) \mu\text{m}/\sqrt{\text{cm}}$, which is higher than the expected value
 274 $236 \pm 3 \mu\text{m}/\sqrt{\text{cm}}$ from a Magboltz calculation [15]. The quoted systematic
 275 uncertainty on D_L is rather large and obtained from a fit using $\sigma_{\text{track}} = 25$
 276 μm .

277 A fit to the $B = 1 \text{ T}$ data shown in Figure 6 gives a longitudinal diffusion
 278 coefficient D_L of $(224 \pm 2 \text{ (stat)} \pm 14 \text{ (sys)}) \mu\text{m}/\sqrt{\text{cm}}$. The measured value

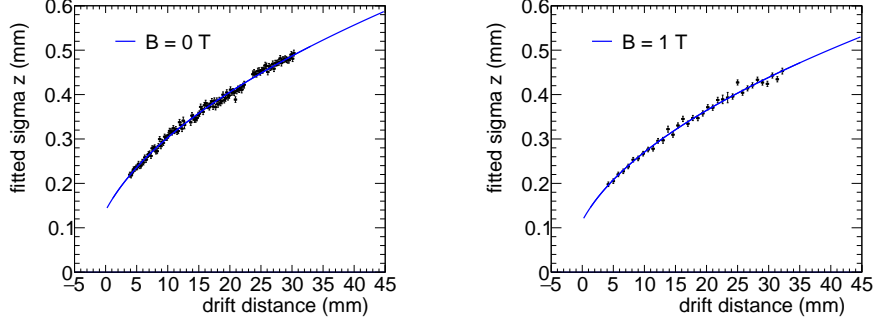


Figure 6: Measured spread on the residuals in the drift plane for hits with a ToT above $0.60 \mu\text{s}$. The data are fitted with the expression of equation (3).

279 is lower than the value of $(245 \pm 4) \mu\text{m}/\sqrt{\text{cm}}$ predicted by Magboltz. The
 280 fitted value of σ_{z0} was $114 \mu\text{m}$.

281 5.3. Deformations in the pixel and drift plane

282 It is important to measure possible deformations in the pixel (xy) and
 283 drift (z) plane to quantify the tracking precision. For the construction of
 284 a large Pixel TPC, deformations in the pixel plane deformation should be
 285 controlled to better than typically $20 \mu\text{m}$ because these affect the momentum
 286 resolution. The mean residuals in the pixel and drift planes are shown in
 287 Figure 7 for the $B = 0 \text{ T}$ data set using a large set of runs to cover the whole
 288 module. The residuals were calculated with respect to the telescope track
 289 prediction. Because of limited statistics, bins were grouped into 8×16 pixels.
 290 Bins with less than 100 hits are left out and residuals larger (smaller) than
 291 $+(-)100 \mu\text{m}$ are shown in red (blue).

292 A few critical areas can be observed in Figure 7: the region around chip 11
 293 is affected (chips 14, 8 and 13), because the grid of chip 11 was disconnected.

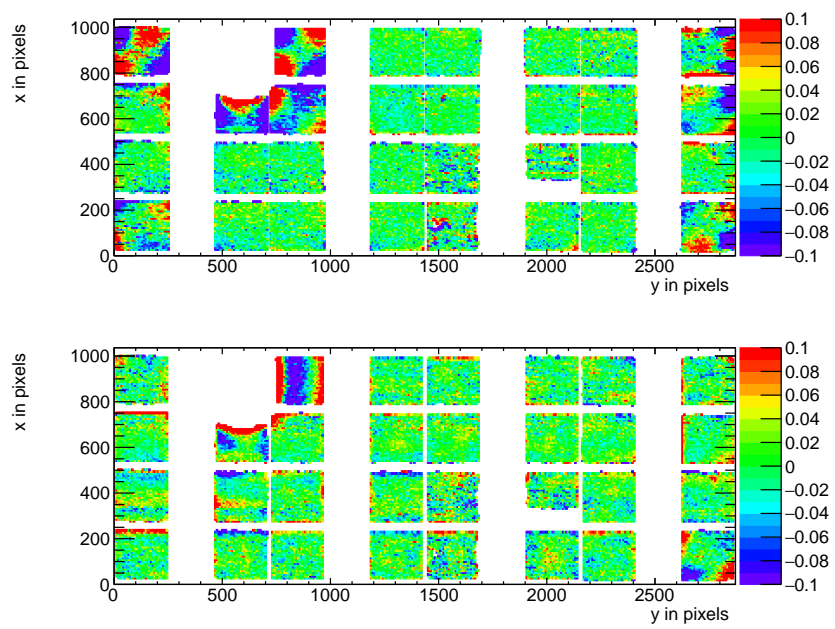


Figure 7: Mean residuals (color coded in mm) in the pixel (top) and drift (bottom) plane for $B = 0$ T data at the expected hit position.

294 Deformations are present at the four corners of the drift box (chips 1, 10, 19
295 and 24) and close to the upper corner edge (chip 16) of the drift box. These
296 come from inhomogenities in the drift field near the supporting pillars, the
297 field wires are too close to the chip to provide a constant electric field. It
298 was concluded that for the deformation studies the hits of these nine chips
299 have to be removed. The track fit was redone leaving these hits out of the fit,
300 such that they could not bias and affect the results. Note that a bias in the
301 mean residual at the edge of the chips is expected to be present for an ideal
302 detector because of the finite coverage and the diffusion in the drift process.

303 In order to reduce the statistical fluctuations and quantify the tracking
304 precision, the module was regrouped in $(4 \times 256) \times 256$ pixel planes put side
305 by side on the horizontal axis, as shown in Figure 8. E.g. the selected chips
306 from the upper left and bottom left quad detectors are superimposed into
307 the 0-256 (x) and 0-256 (y) plane. Bins have a size of 16×16 pixels and bins
308 with less than 1000 entries are not shown. Due to the presence of the dike,
309 pixels at the edge of the chip became covered and inefficient. Therefore, the
310 region of 5 pixels in y near the edge of the chip was removed. For the drift
311 coordinate studies, a region of 10 pixels near the edge of the chip in x and
312 y was removed. The total number of measurements (bins) in xy is 895 and
313 in z 892. One can observe that in the module plane no clear systematic
314 deviations are present and conclude that the guard wire voltages were on
315 average well tuned. Note that in the quad detector module we had no guard
316 wires and deformation corrections had to be applied [2]. The r.m.s. of the
317 distribution of the measured mean residual over the surface in the pixel plane
318 is $11 \mu\text{m}$ and in the drift plane $15 \mu\text{m}$. Similarly, regrouping the module in

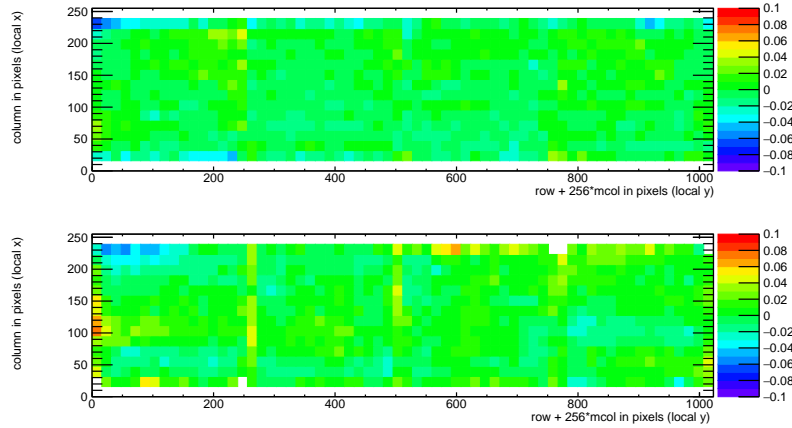


Figure 8: Mean residuals (color coded in mm) in the pixel (top) and drift plane (bottom) for $B = 0$ T data at the expected hit position.

319 $256 \times (4 \times 256)$ pixels put them side by side on the vertical axis, yielded a
 320 r.m.s. in the pixel plane of $13 \mu\text{m}$ and $13 \mu\text{m}$ in the drift coordinate. The
 321 expected statistical error - obtained by propagating the uncertainties on the
 322 residuals - in xy is $4 \mu\text{m}$ and in z $5 \mu\text{m}$.

323 In the $B = 1$ T data set, the electrons will drift mainly along the magnetic
 324 field lines. Deformations are in that case due to e.g. the non-alignment of the
 325 electric and magnetic field, giving $E \times B$ effects. Unfortunately, the statistics
 326 of the telescope tracks that have a matched TPC track was insufficient and
 327 did not cover the full TPC module plane. Therefore the larger statistics of
 328 matched and unmatched TPC tracks was used. TPC tracks were required
 329 to pass angular selection cuts (dx/dy between -40 and -20 mrad and dz/dy
 330 between 0 and 14 mrad) and a momentum cut ($p > 2$ GeV/c and $q < 0$).

331 The mean residuals in the pixel and drift planes are shown in Figure 9 for
 332 the $B = 1$ T data set using a large set of runs to cover the whole module. The

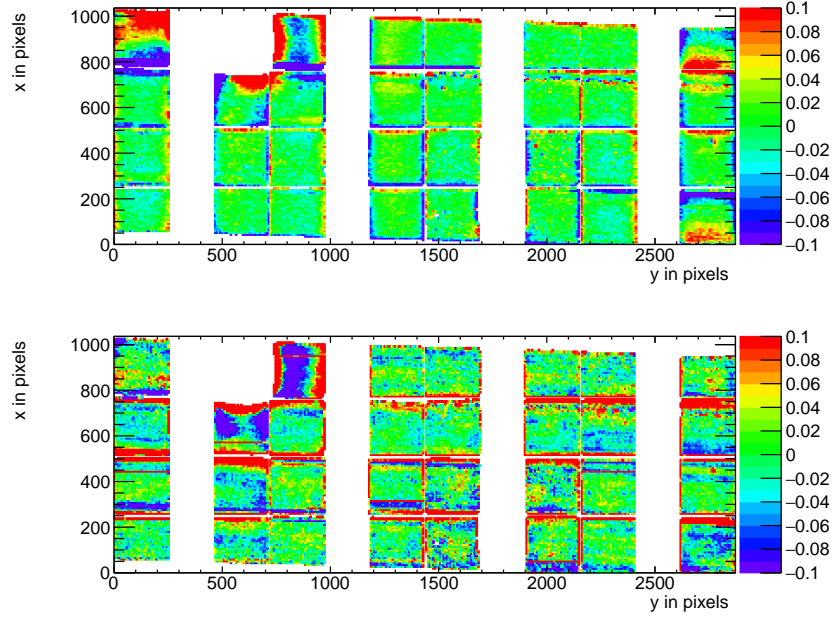


Figure 9: Mean residuals (color coded in mm) in the pixel and drift plane for $B = 1$ T data at the expected hit position.

333 (biased) residuals were calculated with respect to the TPC track prediction.
 334 Because of limited statistics, bins were grouped into 16×16 pixels. Bins with
 335 less than 100 hits are left out and residuals larger (smaller) than $+(-)100 \mu\text{m}$
 336 are shown in red (blue).

337 In Figure 9 the critical areas discussed above - around chip 11, the four
 338 corner chips and chip 16 in the upper corner edge - can be clearly observed.
 339 For the deformation studies, the hits of these nine chips were removed. The
 340 TPC track fit was redone leaving these hits out of the fit, thus that they could
 341 not bias and affect the results. The TPC plane is well covered, although one
 342 can observe that due to the angle of the beam in the xy plane the chips in
 343 the upper right and lower left corners are not fully covered.

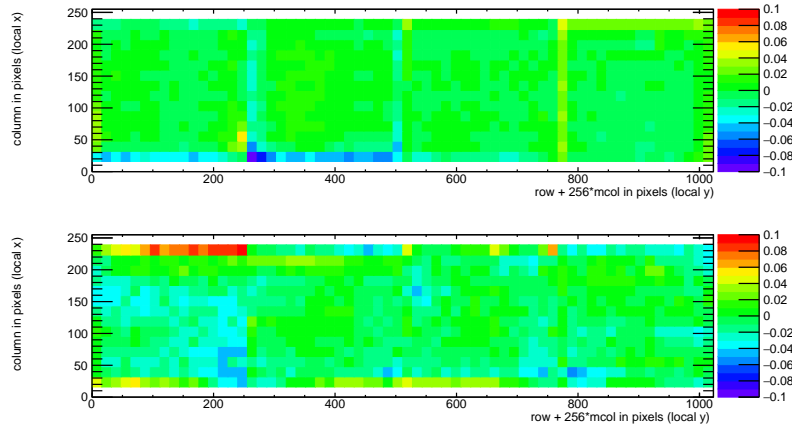


Figure 10: Mean residuals (color coded in mm) in the pixel and drift plane for $B = 1\text{T}$ data at the expected hit position.

344 In order to reduce the statistical fluctuations and quantify the tracking
 345 precision, the module was again regrouped in $(4 \times 256) \times 256$ pixels as de-
 346 scribed above, as shown in Figure 10. Bins have a size of 16×16 pixels and
 347 bins with less than 1000 entries are not shown. Similar to the no-field defor-
 348 mations studies, acceptance cuts had to be applied. The region of 16 pixels
 349 in y near the edge of the chips was removed. For the drift coordinate studies,
 350 in addition a region of 10 pixels in x near the edge of the chip was removed.
 351 The total number of measurements (bins) in xy is 896 and in z 896. One can
 352 observe that in the module plane no clear systematic deviations are present.
 353 The r.m.s. of the distribution of the measured mean residual over the surface
 354 in the pixel plane is $13 \mu\text{m}$ and in the drift plane $19 \mu\text{m}$. Similarly, regroup-
 355 ing the module in $256 \times (4 \times 256)$, yielded a r.m.s. in the pixel plane of $11 \mu\text{m}$
 356 and $20 \mu\text{m}$ in the drift coordinate. The expected statistical error in xy is 2
 357 μm and in z $3 \mu\text{m}$.

358 In summary, the deformations studies for the $B = 0$ and 1 T data demon-
359 strate that the systematical uncertainties in xy are smaller than $13 \mu\text{m}$ with
360 and without magnetic field. The systematical uncertainties in z were smaller
361 than $15 \mu\text{m}$ ($B = 0$ T) and $20 \mu\text{m}$ ($B = 1$ T).

362 5.4. Tracking resolution

363 A selected TPC track in the $B = 0$ T data has on average 1000 hits. The
364 tracking precision in the middle of the TPC (at $y = 1436$ pixels) was derived
365 on a track-by-track basis, by propagating the pixel TPC hit uncertainties. It
366 was found to be on average $9 \mu\text{m}$ in the precision plane and $13 \mu\text{m}$ in z . The
367 angular resolution in dx/dy was on average 0.19 mrad and for dz/dy 0.25
368 mrad. It is clear that the position resolution in the TPC in the precision
369 and drift coordinates is impressive for a track length of (only) 158 mm.
370 The values are smaller than the uncertainty on the track prediction from
371 the silicon telescope of $26 \mu\text{m}$ in x and z on average that is dominated by
372 multiple scattering.

373 6. Single electron efficiency

374 The distribution of the number of TPC track hits per chip - without
375 requiring a matched telescope track - are shown in Figure 11 for the data
376 without magnetic field and for the $B = 1$ T data. For the $B = 0$ T data, the
377 central chips 2,6,7,9,16,17,26 and 27 were selected. For the $B = 1$ T data,
378 the same chips plus chips 12,13,20 and 21 were selected.

379 The mean number of hits is measured to be 124 and 89 in the $B = 0$ T
380 and 1 T data sets respectively. The most probable values are respectively
381 87 and 64. Note that the $B = 0$ T data have a much larger Landau-like

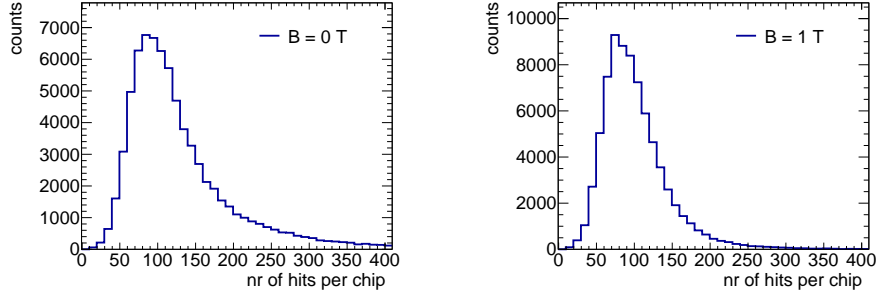


Figure 11: Distribution of the number of TPC track hits per chip for $B = 0$ T (left) $B = 1$ T data.

382 tail than the 1 T data. Also the fluctuations in the core of the distribution
 383 are larger. The mean time over threshold (ToT) is $0.68 \mu\text{s}$ for the $B = 0$ T
 384 and $0.86 \mu\text{s}$ at a $B = 1$ T data. A typical ToT distribution can be found
 385 in Figure 5.5 of ref.[4]. The time over threshold is related to the deposited
 386 charge. This means that the deposited charge per pixel is smaller for the 0
 387 T data. The most probable value for the total deposited charge is similar for
 388 both data sets. A possible explanation for this behavior is that because of
 389 the reduced transverse diffusion in the $B = 1$ T data, the possibility of two
 390 primary electrons ending up in a single grid hole is higher. The mean number
 391 of hits is in agreement with the prediction of 106 electron-ion pairs for a 5
 392 and 6 GeV/c electron at $B = 0$ T for the T2K gas by [13], crossing 236 pixels
 393 or 12.98 mm and a detector running at 85% single electron efficiency. The
 394 measured single electron efficiency at this working point is in agreement with
 395 the efficiency vs mean time over threshold curve that was measured using a
 396 Fe source [4].

397 **7. Conclusion and outlook**

398 A TPC module with 32 GridPix chips was constructed and the perfor-
399 mance was measured using data taken in a testbeam at DESY in 2021. The
400 TPC could be operated reliably and used a 93.6/5.0/1.4 gas mixture (by vol-
401 ume) of Ar/iC₄H₁₀/CO₂ with a small amount of oxygen and water vapour.
402 The analysed data were taken at electron beam momenta of 5 and 6 GeV/c
403 and at magnetic fields of 0 and 1 T.

404 The result for the transverse diffusion coefficient D_T is (287.2 ± 0.5)
405 $\mu\text{m}/\sqrt{\text{cm}}$ at $B = 0$ T and D_T is (120.3 ± 0.5) $\mu\text{m}/\sqrt{\text{cm}}$ at $B = 1$ T. The
406 longitudinal diffusion coefficient D_L is measured to be (251 ± 14) $\mu\text{m}/\sqrt{\text{cm}}$
407 at $B = 0$ T and (224 ± 14) $\mu\text{m}/\sqrt{\text{cm}}$ at $B = 1$ T. Results for the tracking
408 systematical uncertainties in xy were measured to be smaller than 13 μm
409 with and without magnetic field. The tracking systematical uncertainties in
410 z were smaller than 15 μm ($B = 0$ T) and 20 μm ($B = 1$ T).

411 The mean number of hits is in agreement with the predictions of [13] and
412 a detector running at 85% single electron efficiency.

413 Not all data were analysed and users are welcome to study them using
414 the data sets on available on the Grid.

415 The GridPix detector will be further tested and developed in view of a
416 TPC that will be installed in a heavy ion experiment at the EIC or other
417 future colliders. A follow up paper is in preparation on the measured dE/dx
418 or dN/dx resolution and other performance topics.

419 **Acknowledgements**

420 This research was funded by the Netherlands Organisation for Scientific
421 Research NWO. The authors want to thank the support of the mechanical
422 and electronics departments at Nikhef and the detector laboratory in Bonn.
423 The measurements leading to these results have been performed at the Test
424 Beam Facility at DESY Hamburg (Germany), a member of the Helmholtz
425 Association (HGF).

426 **References**

427 [1] C. Ligtenberg, et al., Performance of a GridPix detector based
428 on the Timepix3 chip, Nucl. Instrum. Meth. A 908 (2018) 18–23.
429 arXiv:1808.04565, doi:10.1016/j.nima.2018.08.012.

430 [2] C. Ligtenberg, et al., Performance of the GridPix detector quad,
431 Nucl. Instrum. Meth. A 956 (2020) 163331. arXiv:2001.01540,
432 doi:10.1016/j.nima.2019.163331.

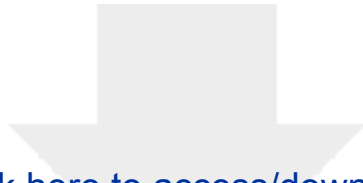
433 [3] J. Kaminski, Y. Bilevych, K. Desch, C. Krieger, M. Lupberger, GridPix
434 detectors - introduction and applications, Nucl. Instrum. Meth. A845
435 (2017) 233–235. doi:10.1016/j.nima.2016.05.134.

436 [4] C. Ligtenberg, A GridPix TPC read out for the ILD experiment at the
437 future International Linear Collider, Ph.D. thesis, Free University of
438 Amsterdam (2021).

439 URL https://www.nikhef.nl/pub/services/biblio/theses_pdf/thesis_C.Ligtenberg.p

- 440 [5] M. Lupberger, Y. Bilevych, H. Blank, D. Danilov, K. Desch, A. Hamann,
441 J. Kaminski, W. Ockenfels, J. Tomtschak, S. Zigann-Wack, To-
442 ward the Pixel-TPC: Construction and Operation of a Large Area
443 GridPix Detector, IEEE Trans. Nucl. Sci. 64 (5) (2017) 1159–1167.
444 doi:10.1109/TNS.2017.2689244.
- 445 [6] T. Poikela, J. Plosila, T. Westerlund, M. Campbell, M. De Gaspari,
446 X. Llopart, V. Gromov, R. Kluit, M. van Beuzekom, F. Zappone,
447 V. Zivkovic, C. Brezina, K. Desch, Y. Fu, A. Kruth, Timepix3: a 65K
448 channel hybrid pixel read out chip with simultaneous ToA/ToT and
449 sparse read out, JINST 9 (05) (2014) C05013.
450 URL <http://stacks.iop.org/1748-0221/9/i=05/a=C05013>
- 451 [7] J. Visser, M. van Beuzekom, H. Boterenbrood, B. van der Heijden, J. I.
452 Muñoz, S. Kulis, B. Munneke, F. Schreuder, SPIDR: a read-out system
453 for Medipix3 & Timepix3, Journal of Instrumentation 10 (12) (2015)
454 C12028. doi:10.1088/1748-0221/10/12/C12028.
- 455 [8] B. van der Heijden, J. Visser, M. van Beuzekom, H. Boterenbrood,
456 S. Kulis, B. Munneke, F. Schreuder, SPIDR, a general-purpose read out
457 system for pixel ASICs, JINST 12 (02) (2017) C02040. doi:10.1088/1748-
458 0221/12/02/C02040.
- 459 [9] F. Hartjes, A diffraction limited nitrogen laser for detector calibration
460 in high energy physics, Ph.D. thesis, University of Amsterdam (1990).
461 URL https://www.nikhef.nl/pub/services/biblio/theses_pdf/thesis_F_Hartjes.pdf
- 462 [10] R. Diener et al., The DESY II test beam facility, Nuclear Instru-

- 463 ments and Methods in Physics Research. Section A: Accelerators, Spec-
464 trometers, Detectors and Associated Equipment 922 (2019) 265–286.
465 arXiv:1807.09328, doi:10.1016/j.nima.2018.11.133.
- 466 [11] P. Baesso, D. Cussans, J. Goldstein, , Journal of Instrumentation 14 (09)
467 (2019) P09019–P09019. arXiv:2005.00310.
468 URL <https://doi.org/10.1088/1748-0221/14/09/p09019>
- 469 [12] D. Dannheim, K. Dort, L. Huth, D. Hynds, I. Kremastiotis, J. Kröger,
470 M. Munker, F. Pitters, P. Schütze, S. Spannagel, T. Vanat, M. Williams,
471 , Journal of Instrumentation 16 (03) (2021) P03008. doi:10.1088/1748-
472 0221/16/03/p03008. arXiv:2011.12730.
473 URL <https://doi.org/10.1088/1748-0221/16/03/p03008>
- 474 [13] R. Veenhof, Garfield - simulation of gaseous detectors, version 9, Refer-
475 ence W5050 (1984-2010).
476 URL <https://garfield.web.cern.ch>
- 477 [14] C. Kleinwort, General broken lines as advanced track fitting method,
478 Nuclear Instruments and Methods in Physics Research Section A: Accel-
479 erators, Spectrometers, Detectors and Associated Equipment 673 (2012)
480 107–110. doi:10.1016/j.nima.2012.01.024.
- 481 [15] S. F. Biagi, Monte Carlo simulation of electron drift and diffusion
482 in counting gases under the influence of electric and magnetic fields,
483 Nucl. Instrum. Meth. A421 (1-2) (1999) 234–240. doi:10.1016/S0168-
484 9002(98)01233-9.
485 URL <https://magboltz.web.cern.ch/magboltz>



Click here to access/download

LaTeX Source Files (Revised and Final)
elsarticle-template-num.tex

